Fabrication and characterization of DIACELL diamond-based detectors for *in vitro* cellular radiobiology

G. Peroni[1], L. Pacher[1,2], V. De Nadal[3], M. Campostrini[3], P. Aprà[1,2], A. Re[1,2], A. Lo Giudice[1,2], L. Guidorzi[1,2], P. Olivero[1,2], R. Cherubini[3], N. Cartiglia[1,2], V. Rigato[3], F. Picollo[1,2]

[1] *Physics Department, Università di Torino, Torino, Italy.* [2] *INFN Sezione di Torino, Torino, Italy.*
[3] *INFN, Laboratori Nazionali di Legnaro, Legnaro (Padova), Italy.*

INTRODUCTION

During the last years, the authors developed innovative diamond-based biosensors for applications in cellular neuroscience. The application of these devices, with embedded graphitic micro-channels, has helped to achieve substantial results in this scientific field. Indeed, for the first time, a correlation between X-rays exposure and the increase of the neurosecretion activity of *in vitro* cellular samples was demonstrated [1].

Electrons generated by ionizing radiation in target biological samples release their energy, and thus damage the chemical structure of the target sample. In radiation biology, the main effects are given by the interaction with DNA. As a consequence, a series of pathways and systems in the cell are activated to efficiently repair the DNA-base damages, even though the excessive damage could eventually lead to the programmed cellular death (apoptosis). For this reason, measurements of the dose delivered to the irradiated cellular samples are crucial to acquire information about the produced damages.

In this framework, the DIACELL project was proposed with the target of developing a device devoted to perform radiobiological experiments, measuring the signals released from the cellular samples during the irradiation, while, simultaneously, detecting the ionizing radiation impinging on the biological samples, in order to quantify the dose delivered to the cells (Fig. 1.a). These devices have been realised using artificial diamond samples since this material presents outstanding properties for biosensing and dosimetric applications [2].

In this paper, we report the fabrication process and the characterization of the latest generation of devices.

DEVICE MICROFABRICATION

Detector-grade single-crystal diamonds produced with the CVD growth technique were used as substrates for the device microfabrication. The samples are classified as type IIa, being characterized by a concentration of nitrogen and boron both lower than 1 ppb, while their size is 4.5×4.5 mm^2 with a thickness of ~60 µm.

These samples were processed with Ion Beam Lithography (IBL) at the AN2000 accelerator of the INFN Legnaro National Laboratories to realize embedded graphitic micro-channels. The IBL technique takes advantage of the metastable nature of the diamond and represents the ideal approach to fabricate the desired conductive structures. Through this technique, structural defects inside the diamond crystal lattice are caused by the nuclear interaction between the accelerated ions and the carbon atoms, entailing chemical, physical and electrical changes into the target. At the end of the range of the ions, a network of sp^2 bonds is formed in correspondence of the Bragg peak. Here, at high irradiation fluences, the concentration of defects exceeds the so-called *graphitization threshold* ($5 \div 9 \times 10^{22}$ vacancies cm^{-3}), which represents a critical damage density at which the formation of the amorphous carbon takes place.

Using 100 µm thick copper masks, manufactured by Kirana (Fig. 1.b), it is possible to implant an array of micro-channels in a parallel approach, thus creating 16 biosensing electrodes for the cellular activity recording (for further information, see [3]) on one side of the diamond, while, on the other side, the necessary number of channels for the corresponding dosimetric measurements. In both cases, the channels are localized at a specific depth below the sample surface. A 1 MeV He^+ ion irradiation at a fluence of 1×10^{17} cm^{-2} was employed to obtain the biosensing channels (~20 µm width, 1.4÷1.9 mm length and ~250 µm thick) at a depth of ~1 µm.

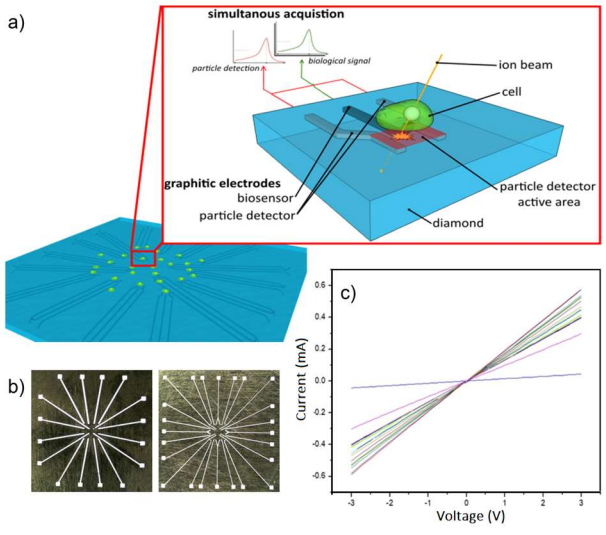

Fig. 1. a) Schematic representation of the DIACELL device. In the red box, two dosimetric electrodes are reported beside the biosensing electrode, as well as the produced electric field. b) Implantation masks. c) I-V characterization of the 16 biosensing electrodes.

A 1.8 MeV He^+ ion irradiation was carried out at the same fluence to realize the dosimetric channels at a depth of ~3 µm. The distance between the planes with the biosensing and the dosimetric electrodes is therefore ~55 µm.

Focused Ion Beam (FIB) micromachining was successively employed to expose to the diamond surface the central and the peripherical areas of the biosensing electrodes. It is worth noting that only the peripherical areas of the dosimetric electrodes need to be exposed, since the central regions are needed to produce a local electric field to detect ionizing radiation. A high-temperature thermal treatment in vacuum at 950 °C for 2 h was performed to convert the amorphous carbon into graphite and the electric characterization of the biosensing channels was performed to verify the quality of the implantation. The current-voltage curves were measured sweeping the voltage between -3 V and +3 V at 0.1 V steps. The biosensing channels exhibited ohmic electrical characteristics (Fig. 1.c). The estimated resistivity values were characteristic of polycrystalline graphite, i.e. ρ_g=(1÷4) mΩ cm, except for one channel, whose low conductivity was probably caused by the accidental definition of its narrower geometry.

ELECTRONICS BOARD

Suitable electronics to collect the biological and the dosimetric data is needed (Fig. 2). The TOFFEE chip [4] was employed to detect the ionizing particles. By connecting a graphitic channel to the high voltage source, a local electric field can be produced between the graphitic channels, and the particle detection can be carried out. For the neurosecretion signals, a LabView-controlled chain composed of a set of amplifiers and an ADC converter was used. The DIACELL sensors were then placed between two chip carriers in order to connect the biosensing and the dosimetric electrodes to the electronics components. A glass ring was glued over one chip carrier to plate the cellular culture.

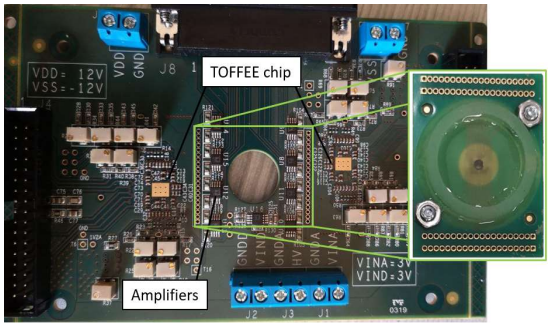

Fig. 2. Electronic board realized for the simultaneous biological sensing and radiation detection. On the right, the final chip with the DIACELL sensor and the chip carriers is shown.

MEASUREMENTS PERFORMED WITH DIACELL SENSORS

DIACELL sensors were used to monitor the cellular secretion of oxidable molecules released from *in vitro* cellular samples. Amperometric experiments with the PC12 cell line were performed in spontaneous and stimulated conditions. By polarizing the electrodes of the biosensors at +800 mV, the secretion activity of the biological samples was recorded, from which the frequency of the exocytotic events was estimated. An example of one amperometric recording is shown in Fig. 3.

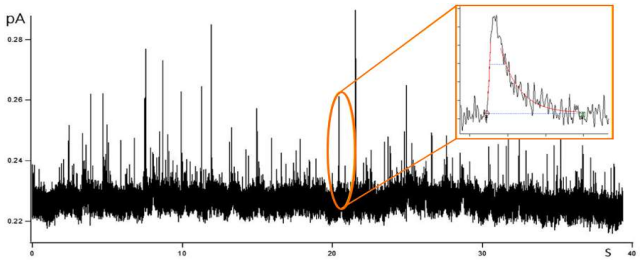

Fig. 3. Typical signal acquired during amperometric measurements.

Moreover, the sensors were employed to detect the ionizing radiation emitted from an X-rays source operating at 500 µA electron current and 150 kV acceleration voltage. Fig. 4.a and Fig. 4.b report the step-like wave output generated from the detection of each particle and the histogram obtained by analysing the time over thresholds of the outputs. In the histogram, both the Bremsstrahlung radiation (orange bins) and the characteristic X-ray lines (blue bins) of the source are observable as two peaks at 4 ns and 6 ns, respectively.

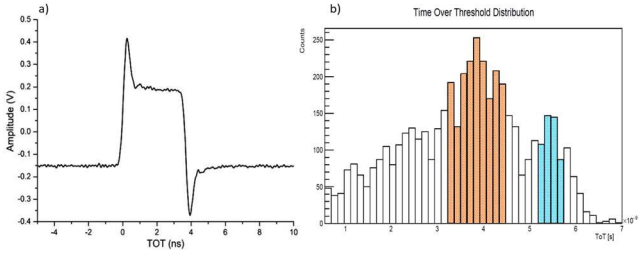

Fig. 4. Step-like wave and histogram collected with the graphitic micro-channels.

CONCLUSIONS

In this report, we described the latest generation of DIACELL integrated biosensor/detector. Their structure has been shown as well as the electronics board necessary to collect the signals.

The devices proved as an efficient tool to perform cellular measurements and to detect ionizing particles and therefore to perform radiobiological experiments.

[1] F. Picollo et al., Nano Lett. *in press* (2020) https://doi.org/10.1021/acs.nanolett.0c01046
[2] V. Carabelli et al., ACS Chem. Neurosci. 8 (2017) 252.
[3] F. Picollo et al., Sci. Rep. 6 (2016) 20682.
[4] F. Cenna et al., Journal of instrum. 12(3) (2017) C03031-C03031